Face milling and turning simulation with the finite element method

L. Masset[*] & J.-F. Debongnie
University of Liège, Manufacturing Laboratory, Chemin des chevreuils 1, 4000 Liège, Belgium
Website : www.ltas19.meca.ulg.ac.be/debongnie/
e-mail : luc.masset@ulg.ac.be; jf.debongnie@ulg.ac.be

P. Beckers
University of Liège, Aerospace Department (LTAS), Chemin des chevreuils 1, 4000 Liège, Belgium
Website : www.ulg.ac.be/ltas-cao/
e-mail : pierre.beckers@ulg.ac.be

ABSTRACT : The paper describes a new simulation tool that gives the machined surface error in face milling and turning. The form error component due to the workpiece flexibility is computed using Samcef finite element code. The finite element analyses are very efficient on industrial applications thanks to the superelement method. Results are obtained in a short time which makes possible a wide range of simulations such as finding the best tool trajectory, testing several tools and cutting conditions and choosing the most suited fixture design.

Key words : finite elements, machining simulation, milling, turning, form error

1 INTRODUCTION

Narrow tolerances are often imposed in automotive engineering, in order to ensure functionality, assembling capabilities or reliability of components such as cylinder heads or transmission casings. The purpose of the research is to develop a tool that computes the workpiece form error of a given machining operation. Such a tool allows to virtually set the process parameters in order to satisfy the tolerances. Some papers describe methods to model machining processes such as cylinder boring [1] and ball-end milling [2]. Like Schulz and Bimschas [3] and Gu *et al.* [4], we consider processes where the main form error component is due to the workpiece flexibility. Here, the finite element (FE) code used to compute the workpiece deformations is Samcef [5].

2 METHOD DESCRIPTION

2.1 Hypotheses

It is assumed that the tool and the machine-tool are perfectly rigid. However some flexibility can be modeled for fixture elements such as back center, screws, supports, … The thermal deformations and the dynamic response of the workpiece are supposed to be small compared to the static deformation. Mill inserts are assumed to be identical and equally spaced.

2.2 Principle

The error of a machined surface point depends on its displacement while the tool is cutting through it. If directed towards the tool, this displacement causes too much material removal. At contrary, if the displacement points towards the workpiece, the tool does not cut enough material. The machined surface error is due to the differences of cut material heights along the surface. A surface point error equals the opposite of its displacement component perpendicular to the surface.

2.3 Application to the finite element method

In this research, we assume that a finite element mesh surface is sufficient to describe the form error. Compared to others [3], the method is much simpler since a time description of the process and complex interpolation algorithms are no more needed.
The principle described in section *2.2* is applied to the surface nodes of the finite element model. For each node we have to compute its displacement while the tool is cutting through it. For that particular tool position the workpiece loads are the clamping forces - constant - and the cutting forces - depending on the tool position. If n is the number of surface nodes, we have to compute n deformed structures by applying n load cases.

2.4 Forces computation

The clamping forces are usually given by the clamping plan. Kienzle's model is used to compute the cutting forces. The three force components, respectively the main cutting force, the feed force and the passive force are given by

$$F_i = b\,h\,k_i \quad \{i = c, f, p\}$$

where b is the width of cut, h is the thickness of cut and k_i is the nominal cutting pressure given by a power law of the thickness $k_i = k_{i\,1.1}\,h^{-m_i}$. Constant values $k_{i\,1.1}$ and m_i for common steels and cast irons were measured König and Essel [6]. For any material, constants can be computed using cutting forces measurements.

2.5 Application of cutting forces on the mesh

The cutting forces are applied on a line γ corresponding to the cutting edge projection on the machined surface (figure 1a). The forces applied by one insert are distributed on N integration points on γ so that

$$F_i = \sum_j^N f_{ij} \quad \{i = c, f, p\}$$

with $f_{ij} = \alpha_j F_i$ and $\sum^N \alpha_j = 1$. Thanks to the load distribution, teeth entries and exits are modeled. Each force f_{ij} is then distributed on the surface element nodes on which it acts (figure 1b). The distribution is performed using the form functions of the surface element. In turning, the forces distribution is similar except that only one tooth is cutting at a time.

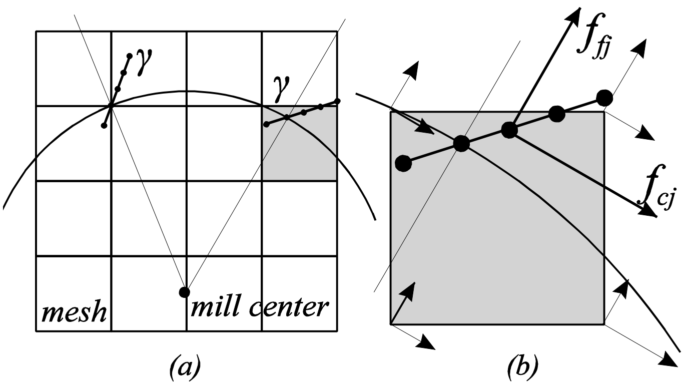

Figure 1 : Cutting edge projection and distributed forces

3 FINITE ELEMENTS ANALYSIS

3.1 Direct method

If n is the number of machined surface nodes, the steps of the direct method are

1. compute the cutting forces for n tool positions and apply them on the mesh nodes;
2. perform the FE analysis (n load cases);
3. build the surface error from the n deformed structures: diagonal picking in the set of displacements vectors

This procedure exhibits two severe drawbacks:

- significant amount of stored data (n load cases)
- high computation cost

Moreover, for each data modification (tool trajectory, cutting conditions, …), a new complete workpiece analysis is required. For these reasons the direct method is uneffective.
As we apply forces only on the surface nodes and as we only use their displacements, a better suited method is the *superelement* one (SE).

3.2 Superelement method

The superelement method consists in building a reduced system - the superelement - by condensing a part of the structure degrees of freedom (d.o.f.). If q_R are the n_R retained degrees of freedom and q_C are the n_C condensed ones, the system $K\,q = g$ can be written in the following way

$$\begin{bmatrix} K_{RR} & K_{RC} \\ K_{CR} & K_{CC} \end{bmatrix} \begin{bmatrix} q_R \\ q_C \end{bmatrix} = \begin{bmatrix} g_R \\ g_C \end{bmatrix}$$

If we assume that all the loads g_C equal to zero, this leads to the reduced system

$$\left[K_{RR} - K_{RC}\,K_{CC}^{-1}\,K_{CR}\right] q_R = g_R \;\Leftrightarrow\; K_{RR}^{*}\,q_R = g_R$$

Here, the retained degrees of freedom are

- the d.o.f. of the machined surface
- the d.o.f. corresponding to other loaded nodes (clamping forces)

The first part of the resolution is to compute the reduced matrix K_{RR}^{*} (SE creation step). Then the inversion of K_{RR}^{*} is performed by applying a unit force in each of the three directions on the n machined surface nodes (SE use step). The $3n$ obtained displacement fields give the flexibility matrix S.

With the SE method, a simulation result is obtained almost directly since it requires only the multiplication of small matrices (dimension $n_R \times n_R$).

3.3 SE method performance

Analyses were performed with Samcef V8 on a standard computer running Windows NT (Pentium III 770 MHz with 512 Mb of memory).Table 1 shows the ratio between the direct and SE methods on small FE models (up to 11295 d.o.f.). Table 2 shows the CPU time and disk space required to obtain the inverted reduced matrix S (both SE creation and SE use steps) on the industrial applications. Even for large models, a very low computation time is necessary thanks to the new sparse solver of Samcef.

Table 1 : Direct and SE method comparison

	CPU	disk
ratio [direct method / SE method]	30 to 50	3 to 5

Table 2 : SE method performance (Samcef V8 with sparse solver)

	d.o.f. (retained)	CPU (s)	disk(Mb)
camshaft cover	36639 (2436)	153	750
suspension support	121749 (1851)	133	683
exhaust manifold	184944 (3087)	397	1578
gear box cover	112365 (5328)	2017	4362

4 CAMSHAFT COVER

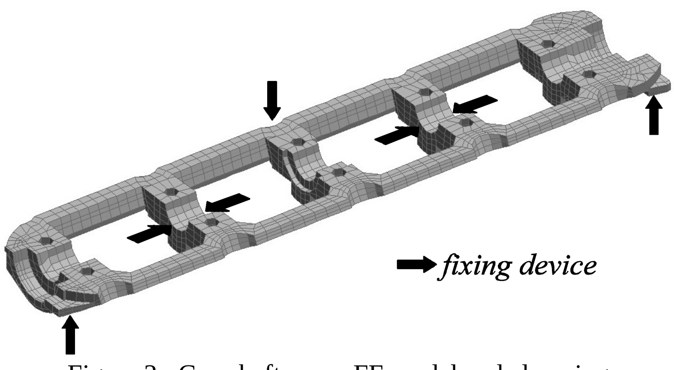

Figure 2 : Camshaft cover FE model and clamping

The workpiece is made of aluminium A-S9U3Y40. Figure 2 shows the FE model and the fixture. The tool is a 100-mm mill with four carbide inserts. The aim of the simulation is to find the trajectory leading to the smallest form error among the two possible centered trajectories. The obtained results are illustrated on figure 3.

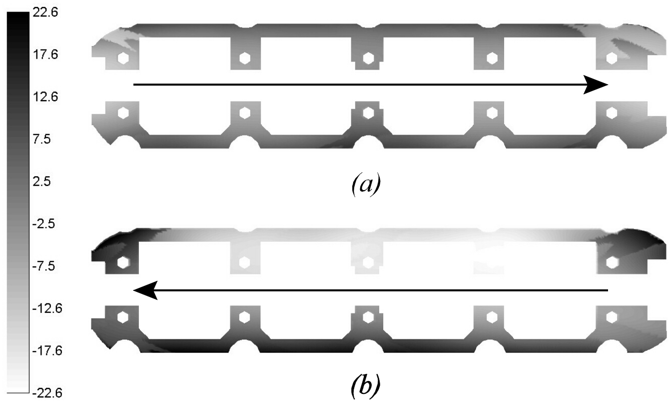

Figure 3 : Flatness errors obtained with trajectories (a) and (b) are equal to 27.4 µm and 45.2 µm respectively

5 SUSPENSION SUPPORT

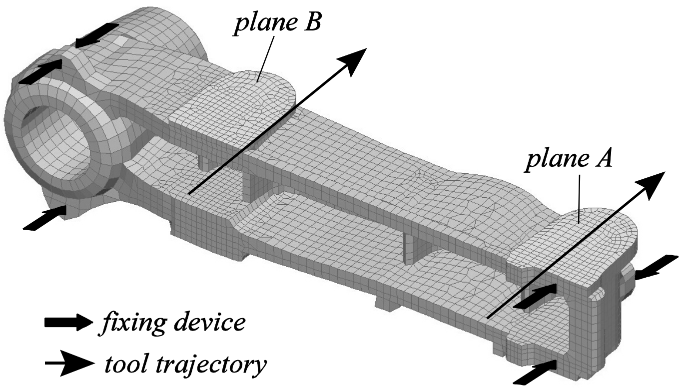

Figure 4 : Suspension support FE model, fixing devices and tool trajectory

The suspension support is made of cast iron GS52 and face milled with the tool trajectory shown on figure 4. Two mills are compared in this simulation: a 100-mm mill with 14 inserts and a 140-mm mill with 10 inserts. Figure 5 shows the results obtained for plane A.

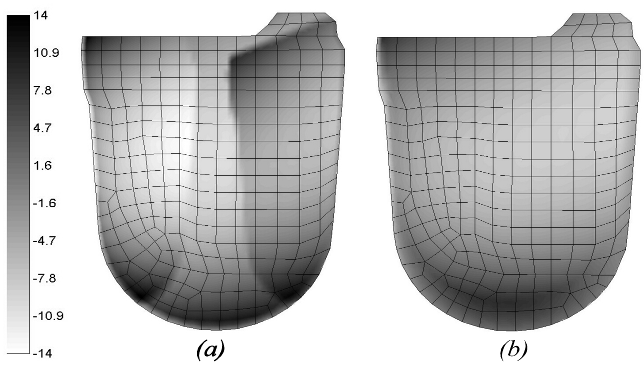

Figure 5 :Flatness errors for plane A with 100-mm mill (a) and 140-mm mill (b) are equal to 27.9 µm and 18 µm respectively

6 EXHAUST MANIFOLD

The material is a cast iron GS53. The tool is a 315-mm mill with 50 inserts. The initial fixture design is shown on figure 6. The four pipes are clamped with strap-support couples.

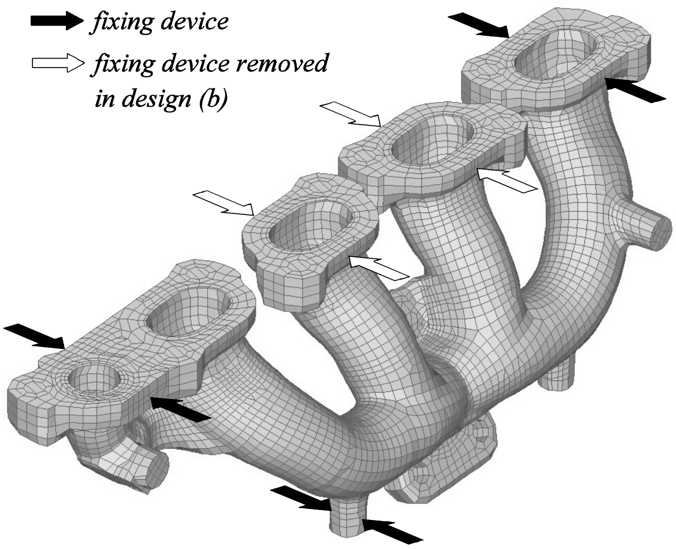

Figure 6 : Exhaust manifold FE model and fixture

The flatness error computed with original clamping design is shown on figure 7a. It is far lower than the tolerance. The idea is to test a lighter fixing whose advantage is that the clamping operation is easier and faster. We remove the fixtures of the two inner pipes because their lengths are smaller than the outer ones. The obtained flatness error is obviously greater than before (figure 7b) but it still satisfies the tolerance.

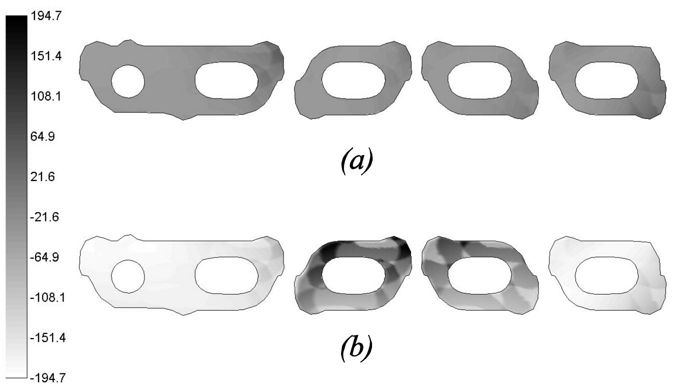

Figure 7 : Flatness errors obtained with fixture design (a) and (b) are equal to 103.9 µm and 389.3 µm respectively

6 GEAR BOX COVER

The process is the transverse turning of a gear box cover made of aluminium A-S9U3Y40. For the finishing pass, the depth of cut equals 0.5 mm. The fixture is constituted of three strap-support couples (figure 8). Here, the simulation purpose is simply to check if the machined surface satisfies the imposed tolerance of 30 µm. The small flatness error obtained (22.8 µm) is due to the very low cutting forces level in aluminium and the small depth of cut in finishing (maximum passive force value equals 24 N).

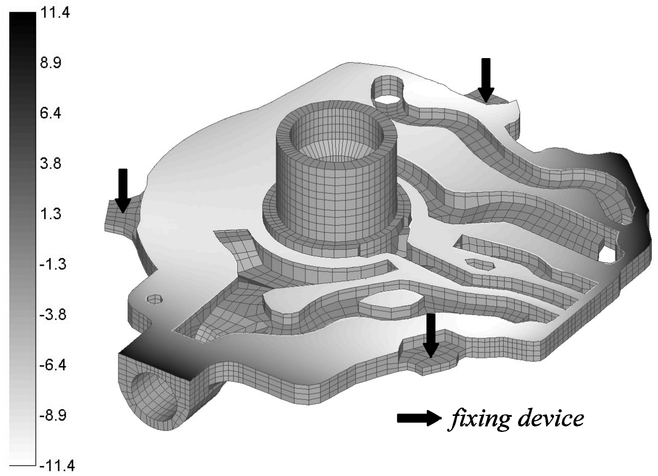

Figure 8 : Gear box cover model and flatness error obtained

7 CONCLUSION

The simulation tool proved to be very flexible and cost effective for industrial applications. The influences of the cutting process parameters are easily shown off in order to choose the best process settings.

Acknowledgments

The authors gratefully acknowledge the financial and technical support of the Renault Department of Powerstrain Structural Analysis, Rueil-Malmaison, France. We would thank the Renault team members, S. Foreau, T. Dumont, J.-J. Droux, J. Duysens and P. Le Roy for their help.

References

[1] Kakade, N. N., Chow, J. G., 1993, *Finite Elements Analysis of Engine Bore Distorsions During Boring Operation*, ASME Journal of Engineering For Industry, Vol. 115, pp. 379-384

[2] Feng, H. Y., Menq, C. H., 1996, *A Flexible Ball-End Milling System Model for Cutting Force and Machining Error Prediction*, ASME Journal of Manufacturing Science and Engineering, Vol. 118, pp. 461-469

[3] Schulz, H., Bimschas, K., 1993, *Optimization of precision Machining by Simulation of the Cutting Process*, Annals of the CIRP, Vol. 42/1, pp. 55-58

[4] Gu, F., Melkote, S. N., Kapoor, S. G., DeVor, R. E., 1997, *A Model for the Prediction of Surface Flatness in Face Milling*, ASME Journal of Manufacturing Science and Engineering, Vol. 119, pp. 476-484

[5] Samcef FE code, *Système d'Analyse des Milieux Continus par la Méthode des Eléments Finis*, www.samcef.com

[6] König, W., Essel, K., 1973, *Spezifische Schnittkraftwerte für die Zerspanung Metallischer Werkstoffe*, Verlag Stahleisen M. B. H., Düsseldorf